Axial magnetic field injection in magnetized liner inertial fusion

Cite as: Phys. Plasmas **24**, 102712 (2017); https://doi.org/10.1063/1.4986640
Submitted: 06 June 2017 • Accepted: 02 October 2017 • Published Online: 31 October 2017

P.-A. Gourdain, M. B. Adams, J. R. Davies, et al.

Axial magnetic field injection in magnetized liner inertial fusion

P.-A. Gourdain,[1] M. B. Adams,[1] J. R. Davies,[2] and C. E. Seyler[3]
[1]*Extreme State Physics Laboratory, Physics and Astronomy Department, University of Rochester, Rochester, New York 14627, USA*
[2]*Laboratory for Laser Energetics, University of Rochester, Rochester, New York 14627, USA*
[3]*Laboratory for Plasma Studies, Cornell University, Ithaca, New York 14850, USA*

(Received 6 June 2017; accepted 2 October 2017; published online 31 October 2017)

MagLIF is a fusion concept using a Z-pinch implosion to reach thermonuclear fusion. In current experiments, the implosion is driven by the Z-machine using 19 MA of electrical current with a rise time of 100 ns. MagLIF requires an initial axial magnetic field of 30 T to reduce heat losses to the liner wall during compression and to confine alpha particles during fusion burn. This field is generated well before the current ramp starts and needs to penetrate the transmission lines of the pulsed-power generator, as well as the liner itself. Consequently, the axial field rise time must exceed hundreds of microseconds. Any coil capable of being submitted to such a field for that length of time is inevitably bulky. The space required to fit the coil near the liner, increases the inductance of the load. In turn, the total current delivered to the load decreases since the voltage is limited by driver design. Yet, the large amount of current provided by the Z-machine can be used to produce the required 30 T field by tilting the return current posts surrounding the liner, eliminating the need for a separate coil. However, the problem now is the field penetration time, across the liner wall. This paper discusses why skin effect arguments do not hold in the presence of resistivity gradients. Numerical simulations show that fields larger than 30 T can diffuse across the liner wall in less than 60 ns, demonstrating that external coils can be replaced by return current posts with optimal helicity. https://doi.org/10.1063/1.4986640

INTRODUCTION

The MagLIF[1] experimental platform developed at Sandia National Laboratories may place pulsed-power drivers at the forefront of fusion research, together with NIF and ITER. MagLIF relies on the implosion of a DT-filled metal liner using >40 MA of current to fulfill Lawson's criterion.[2] The original idea calls for three key elements. First, the liner must be thick enough to avoid magneto-Rayleigh-Taylor instabilities from puncturing the liner. Second, an axial magnetic field is required to quench electron thermal conduction to the liner wall. The axial magnetic field must be compressed by the imploding liner to confine alpha particles at stagnation.[3] Finally, the fuel must be heated just before the implosion starts, in order to reach fusion temperatures at moderate convergence ratios. Generating an initial axial magnetic field of 30 T is one of MagLIF's biggest technical challenges. The Helmholtz coil required to generate this magnetic field takes valuable space near the load, increasing the load inductance. Yet, it seems possible to use small portion of the mega-amperes of current available to generate 30 T field. However, one might expect from the simple linearized theory of magnetic diffusion that the magnetic field can only penetrate the wall by a distance δ, the skin depth, given by

$$\delta = \sqrt{\frac{\eta}{\pi f \mu_0}}. \tag{1}$$

δ is on the order of 50 μm for an aluminum liner with a resistivity η of 2.6×10^{-8} Ω m, at a frequency f of 2.5 MHz (we suppose the current rise of 100 ns is 1/4 of a sine wave). MagLIF calls for a wall thickness on the order of 300 μm to mitigate magneto-Rayleigh-Taylor instabilities. Thus, a magnetic field rising in 100 ns does not have the time to diffuse through the liner on the implosion time scale. This model uses Faraday's law

$$-\frac{\partial \vec{B}}{\partial t} = \vec{\nabla} \times \vec{E}, \tag{2}$$

and Ampere's law in the quasi-static regime,

$$\vec{\nabla} \times \vec{B} = \mu_0 \vec{J}, \tag{3}$$

to predict magnetic field diffusion through conductors. In the resistive limit of Ohm's law, the electric field is directly proportional to the current via the resistivity η

$$\vec{E} = \eta \vec{J}. \tag{4}$$

However, when the resistivity is not homogenous (e.g., caused by large differences in temperature), field diffusion becomes non-linear, and it deviates from the skin effect. In this case, the time evolution of the current density becomes

$$\frac{\partial \vec{J}}{\partial t} - \frac{\eta}{\mu_0}\vec{\nabla}^2\vec{J} + 2\left(\vec{v}_\eta.\vec{\nabla}\right)\vec{J} - \vec{\nabla}\left(\vec{v}_\eta.\vec{J}\right) + \left(\vec{\nabla}.\vec{v}_\eta\right)\vec{J} = 0. \tag{5}$$

We replaced resistivity gradients with an effective velocity

$$\vec{v}_\eta = -\frac{1}{\mu_0}\vec{\nabla}\eta. \quad (6)$$

$\left(\vec{v}_\eta.\vec{\nabla}\right)\vec{J}$ is an advection term with velocity $\vec{v}_\eta$ in Eq. (5). When a liner carries large current densities, like in the Z machine, large temperature variations arising inside the liner cause resistivity gradients. Since the liner is in the warm dense matter (WDM) regime, resistivity gradients can be relatively large.[4,5] The current penetration becomes non-linear and the penetration time can be much shorter than the skin time, with a burn-through velocity, given by Eq. (6). This phenomenon is discussed in greater details by Knoepfel.[6]

This paper proposes to explore this non-linear diffusion effect inside a broader framework, where electron physics is taken into account via the generalized Ohm's, given by

$$\frac{\partial\vec{J}}{\partial t} + \vec{\nabla}.\left(\vec{u}\vec{J} + \vec{J}\vec{u} - \frac{1}{en_e}\vec{J}\vec{J}\right) = \frac{n_e e^2}{m_e}\left(\vec{E} + \vec{u}\times\vec{B} - \eta\vec{J} - \frac{1}{en_e}\left[\vec{J}\times\vec{B} - \vec{\nabla}p_e\right]\right), \quad (7)$$

Electron effects, like Hall and electron inertia, impact greatly the flow of electromagnetic energy, especially near the plasma-vacuum interface. In this framework, the generalized Ampere's law should be used instead

$$\varepsilon_0\mu_0\frac{\partial\vec{E}}{\partial t} = \vec{\nabla}\times\vec{B} - \mu_0\vec{J}. \quad (8)$$

Finally, the equation of state and the mixing of states should also be considered. This paper mostly ignored these effects but dd consider phase transitions and phase mixing inside the liner material. This work uses slanted posts inside the return current path to generate the required magnetic field. Posts are preferred to circular windings since the voltage drop between conductors is smaller.[7] After this introduction, we highlight the main results obtained from numerical simulations and then discuss the implication for MagLIF.

PERSEUS SIMULATIONS

A means to generate an external magnetic field using the current available from the Z machine could simplify platform design and decrease load inductance when axial field coils are removed. For instance, Automag[8] uses a conductive helical path allowing the formation of axial magnetic fields directly inside the liner, eliminating the Helmholtz coil altogether. It was suggested that the helical structure inside the liner does not impact noticeably magneto-Rayleigh-Taylor instabilities.[8] Given the importance of capsule and drive symmetry for all ICF concepts, a pre-magnetization method that eliminates the need to introduce dramatic topological changes in the liner could be extremely beneficial. In this paper, we explore how a helical path machined in the return current can surrounding the liner may achieve the required pre-magnetization. The evaluation of the penetration of the magnetic field across a liner wall was done using the three-dimensional code PERSEUS.[9] The numerical simulations presented here considered the phase transitions of aluminum as well as mixing between solid, liquid, gas, and plasma states.[4] Figure 1 shows the geometry used in the simulations. The domain footprint is 18 mm long by 18 mm wide. Its height is 11 mm with 88 million grid cells ($512\times512\times336$). The geometrical resolution was 40 μm. The resolution is small enough to resolve the room temperature skin depth and large enough to allow for reasonable time steps. The numerical simulation used 4096 processors. The liner is made of aluminum, with a wall thickness of 300 μm and a radius of 3 mm. The initial conditions for density are shown in Fig. 1. The vacuum density is set to be $6\times10^{14}\text{cm}^{-3}$. The temperature is set to 23 °C. All boundary conditions are open except at the anode-cathode gap (indicated by "A-K gap" in Fig. 1) where we imposed a 1/r magnetic field decay, generated by a current rise from 0 to 27 MA. The time evolution of the current

$$I(t) = I_{peak}\sin^2\left(\frac{\pi}{2}\frac{t}{t_r}\right), \quad (9)$$

uses t_r as the current rise time and I_{peak} is the peak current of 27 MA. In this magnetic configuration, the current flows down the liner, from the anode to the cathode. The outer posts are slanted by 0° or 22.5° from the vertical. Since our main focus is the injection of axial field across the liner wall, we chose to keep the liner empty, focusing only on field penetration across the liner wall. There is no thermal conductivity implemented inside PERSEUS, at present. While this can be a potential area of concern for these simulations, we argue in our conclusions that thermal diffusion is too slow inside the liner to play an important role.

AZIMUTHAL MAGNETIC FIELD PENETRATION INTO THICK LINERS

First, we ran a simulation with vertical posts. There is no axial field generation in this case, allowing us to study only the evolution of the azimuthal field. Figure 2(a) shows the magnetic field profile across the liner wall at 6 different times during the current rise, from 10 to 60 ns. The lineout direction is shown in Fig. 1. We do not look at later times when the inner surface of the liner begins to move. The liner

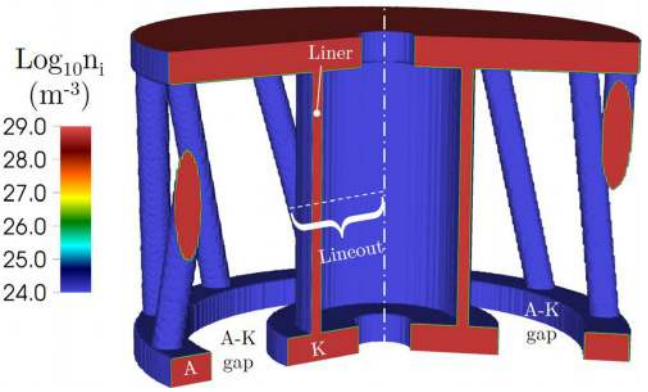

FIG. 1. Overall geometry used in the simulation showing the liner, the anode (A), the cathode (K), and the A-K gap. The lineout used in in other figures is also indicated. The liner radius is 3 mm.

wall starts at a radius of 3 mm and stops at 2.7 mm in these plots. At t = 10 ns, we clearly see that the azimuthal magnetic field penetrated half-way the liner wall. Figure 2(b), at the same point in time, indicates that the current already flows inside the liner wall. This is clearly in complete contradiction with the skin effect argument developed in the introduction. While any resistivity models used in numerical simulations can always be improved, we argue that the effects seen here are mostly caused by non-linear diffusion. At t = 20 ns, we see that the magnetic field has not penetrated deeper inside the liner wall. In fact, even 30 ns after the current starts, the magnetic field has not progressed significantly across the wall. Figure 2(b) shows that the current density peaks at the same location inside the liner wall for the first 50 ns of the current rise. As indicated by Fig. 3, which shows the strength of different vertical electric fields in the region surrounding the liner, the purely Ohmic electric field, $\vec{E} = \eta\vec{J}$, dominates inside the liner. We have not plotted the electric field due to electron inertia which can be deduced by subtracting all other electric fields from the total electric field plotted in Fig. 3. In the panels a through d of Fig. 3, the resistive electric field is the greatest near the edges of the liner wall. The resistivity gradients force the current to flow only in regions of low resistivity, inside a channel located in the center of the liner wall. This status quo is only broken when the plasma ablated from the wall can carry a sizable portion of the current away from the liner wall, happening in the second half of the discharge (t > 50 ns). It is important to note that t = 50 ns is the last time where the inner surface of the liner wall is motionless.

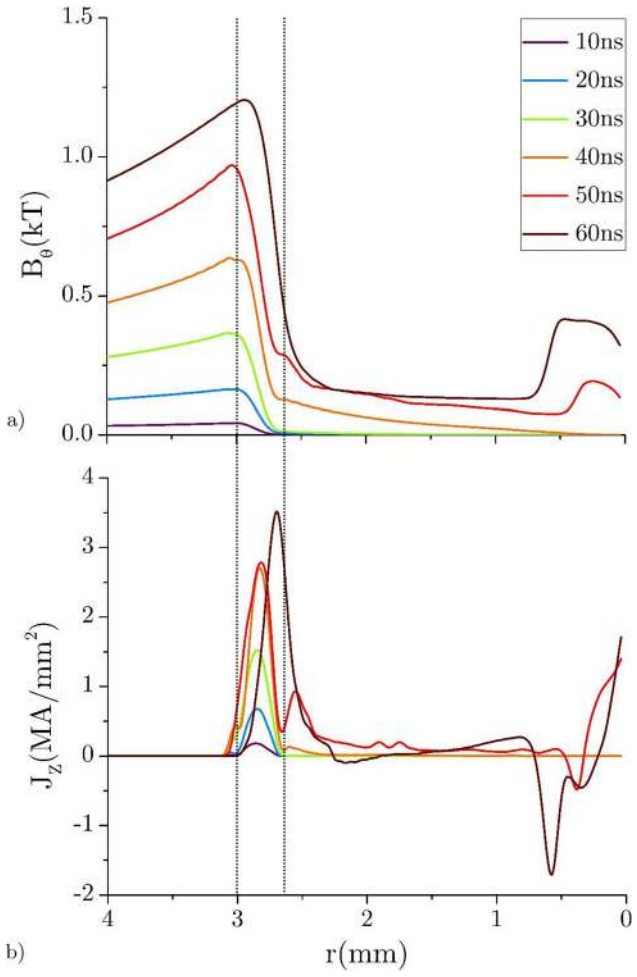

FIG. 2. The time evolution of (a) the azimuthal magnetic field and (b) the axial current density computed by PERSEUS along the lineout indicated in Fig. 1. The vertical lines indicate the initial location of the liner wall.

The Hall and electron pressure electric field, $\vec{E} = \frac{1}{en_e}\left[\vec{J} \times \vec{B} - \vec{\nabla} p_e\right]$, contribute very little to the total electric field. Early in time [Figs. 3(a) and 3(b)], the two major sources of electric fields are electron inertia in the low-density regions (r > 3 mm and r < 2.7 mm) and resistivity. Once the liner starts to be compressed and plasma ablation becomes dominant near the wall, the dynamo electric field, $\vec{E} = -\vec{u} \times \vec{B}$, becomes another important source of electric fields. In fact, the dynamic of the magnetic field is dominated by dynamo in the low-density regions early in time (t > 20 ns) and across the whole domain at later times (t > 60 ns). Before 40 ns, there are no visible large-scale variations of the vertical electric field along the radial direction except for minor two-fluid plasma instabilities responsible for oscillations of the electric field outside the liner wall. After t = 40 ns, the vertical electric field starts to vary with the radius, causing a change in magnetic field inside the liner bore.

For good measure, we compare our simulations with measurements done on the Z machine using a beryllium liner.[10] Beryllium has a resistivity similar to aluminum, giving a skin depth on the order of 50 μm. Experimental data in Ref. 10 show that an azimuthal magnetic field can be measured inside the liner after 100 ns, clearly showing that the skin effect model does not apply to such experimental conditions. Our simulations find that the azimuthal field has fully penetrated the liner after only 40 ns. This value is in good agreement with the experiment since our liner is half the thickness of the beryllium liner imploded on Z.[10]

AXIAL MAGNETIC FIELD PENETRATION INTO THICK LINERS

Now the simulation was run with posts slanted by 22.5°, as shown in Fig. 1. The penetration of the azimuthal magnetic field in this new configuration is virtually unchanged compared to the case where the posts are vertical. We expect the axial magnetic field to penetrate as quickly as the azimuthal field. We have verified that the azimuthal magnetic field penetration is virtually identical in both configurations. Consequently, we did not plot the azimuthal field profile across the wall in this case. Figure 4(a) shows the axial magnetic field along the lineout defined in Fig. 1. The field inside the liner steadily grows to 30 T, 50 ns into the current discharge. It reaches 70 T when the inner surface of the liner starts to move, 60 ns into the current discharge. Most of the azimuthal currents flow inside the wall by now. As its axial counterpart, the currents flow in the region of lowest resistivity, at the center of the liner wall, not at its edge as it would happen in usual linear magnetic diffusion. Such current distribution yields a constant magnetic field inside the bore of the liner, except near the axis, caused by the migration of a small portion of the field across the liner bore.

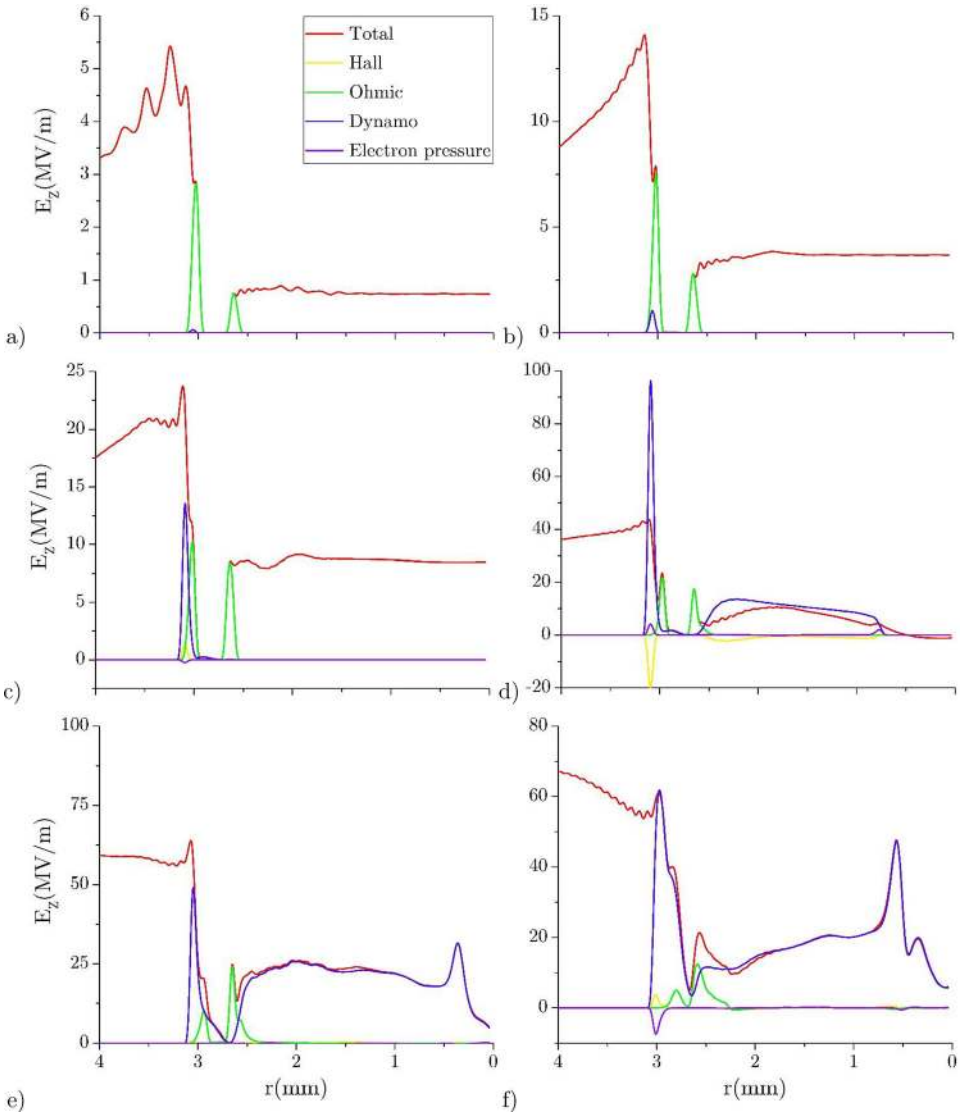

FIG. 3. The total, Hall, Ohmic, dynamo, and electron pressure vertical electric fields at (a) 10 ns, (b) 20 ns, (c) 30 ns, (d) 40 ns, (e) 50, and (f) 60 ns along the line-out indicated in Fig. 1.

Figure 5(a) shows the plasma ion density, 70 ns into the current discharge. At this point in time, the inner surface of the liner just started to move. The plasma from the inner surface of the liner has reached the axis. This potentially raises issues since the liner material could mix with the fusion fuel as early as 70 ns into the discharge. Figure 5(b) shows that the plasma on axis is relatively hot compared to the liner wall. The current mostly flows in three different regions: electrodes, liner, and near the axis, as shown in Fig. 5(c). The current flowing inside the liner bore is carried by the ablated plasma from the inner wall. This plasma could mix with the fuel, a situation that should be avoided. However, it also indicates that the axial field has penetrated the liner. It is clear from Fig. 5(d) that the axial field plotted along a single lineout in Fig. 4 is present in the whole volume surrounding the liner, demonstrating that axial field injection can be used to pre-magnetize MagLIF targets using a portion of the current discharge generated by the Z machine.

DISCUSSION

Numerical simulations have shown that skin effects can be largely ignored in MagLIF. Non-linear diffusion is the dominant mechanism and speeds up the penetration of the magnetic field across the liner wall. We argue that this penetration is mostly caused by resistivity gradients, at least during the first 40 ns. Figures 3(a)–3(d) show that only Ohmic electric fields dominate inside the liner wall. We can estimate the impact of linear diffusion (i.e., skin effect) with respect to non-linear diffusion by looking at the ratio of these two main terms of Eq. (5). An order of magnitude for this ration is given by

$$\frac{\frac{\eta}{\mu_0}\vec{\nabla}^2\vec{J}}{\left(\frac{1}{\mu_0}\vec{\nabla}\eta.\vec{\nabla}\right)\vec{J}} \sim \frac{L_\eta}{L_J}. \tag{10}$$

L_J is the scale length of current gradients (i.e., the skin depth δ) and L_η is the characteristic scale length of the resistivity gradients. In this calculation, we use $\Delta^2 J/\Delta J \sim 1$, since we look at gradients across regions where ΔJ is large and regions where ΔJ is 0 (since $J \sim 0$ there). In our study, the resistivity in the warm dense matter state is also relatively large[5] compared to the resistivity at room temperature and $\Delta\eta/\eta \sim 1$ also holds here. When the scale length of the

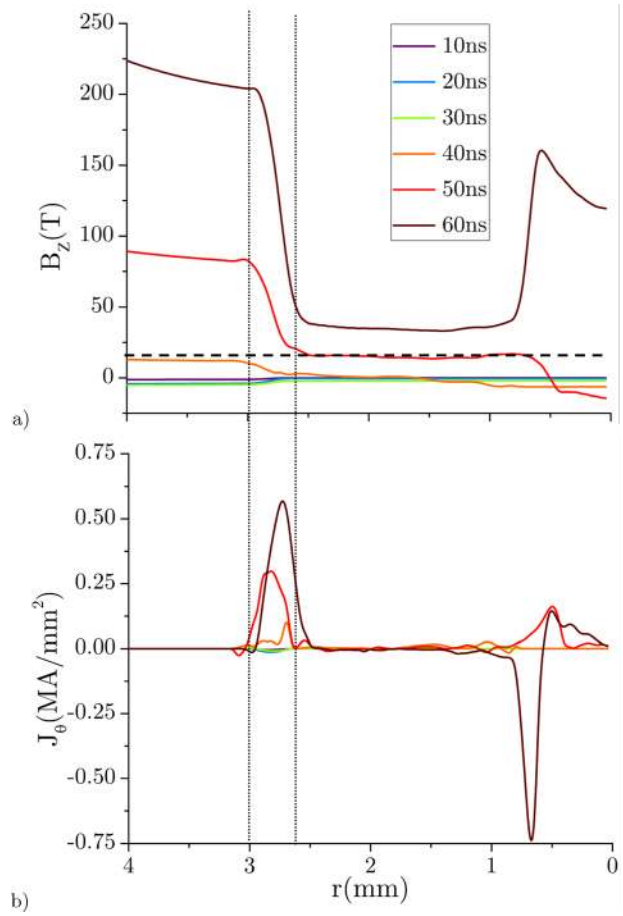

FIG. 4. The time evolution of (a) the axial magnetic field and (b) the azimuthal current density computed by PERSEUS along the lineout indicated in Fig. 1. The vertical lines indicate the initial location of the liner wall. The horizontal dashed line corresponds to 30 T, the nominal axial field required by the MagLIF concept.

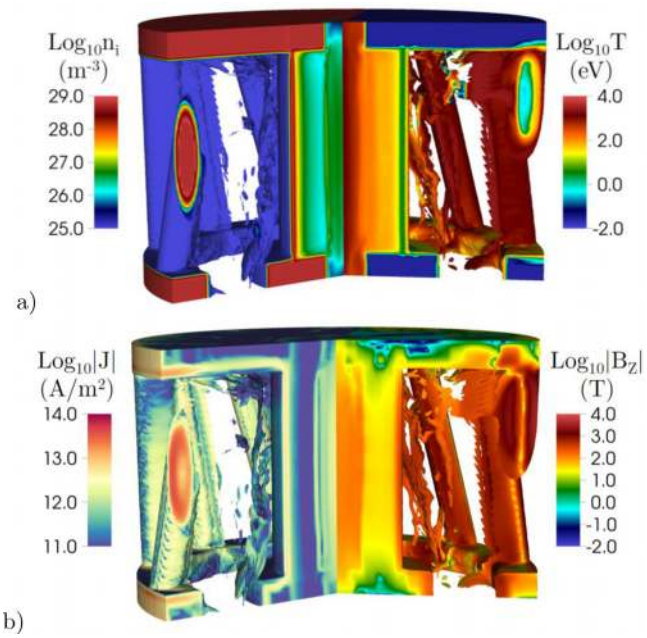

FIG. 5. (a) Ion density (left) and temperature (right) on a $\log_{10}$ scale, (b) current density (left) and magnetic field (right), on a $\log_{10}$ scale, at 70 ns when the liner starts to implode. Regions where ion density is below $10^{25}\,m^{-3}$ are not displayed.

resistivity gradients is much smaller than the skin depth, then the non-linear diffusion term in Eq. (5) prevails over the linear diffusion term. We are in this case here. L_η will always be smaller than L_J since it takes some time, after the current penetrates to heat up the material and change the resistivity. The time t_η required for current redistribution can be estimated using

$$t_\eta \sim \frac{L_\eta}{v_\eta} \sim \mu_0 \frac{L_\eta^2}{\Delta\eta}. \tag{11}$$

This time is not related to the skin time. To get an upper bound for t_η, we can assume $L_\eta \sim \delta$ and we find that the time required for the current to move from a region of high resistivity to a region of lower resistivity is on the order of several nanoseconds. Figure 2(b) confirms that the redistribution of the current happens in 10 ns and stays the same for the next 40 ns. In conclusion, the time it takes for the current to penetrate the liner is controlled by heat capacity and heat conduction rather than the current rise time.

This paper oversimplified these effects and they should be studied independently to evaluate the current penetration inside the liner wall. Thermal conductivity can smooth out thermal gradients and reduce resistivity gradients. However, it is important to note that a thermal conductivity larger than 1 MW/m/K is required to impact noticeably the temperature profiles at 50 eV. It is reported to be 1 kW/m/K at 2 eV.[11,12] We have also ignored thermo-electric effects, given by $\vec{E}_{th} = k\boldsymbol{\beta} \cdot \vec{\nabla} T_e/e$ where $\boldsymbol{\beta}$ is the thermoelectric tensor. Comparing the advection speed v_N of the Nernst effect with the resistive advection speed v_η, we get $v_N/v_\eta \approx v_{e_{th}}^2 / \left(\delta_e^2 \left[\nu_{ee}^2 + \omega_{ce}^2\right]\right)$, where v_e is the electron thermal speed, δ_e is the electron skin depth, ν_{ee} is the electron-electron collision frequency, and ω_{ce} is the electron cyclotron frequency. For conditions of interests, electrons in the liner are not magnetized. We can then approximate this ratio to $v_N/v_\eta \approx 10^4 T_{keV}^4/n_{27}$ using Eqs. (30), (34), (36), and (38) from Ref. 13. Here, n_{27} is the electron number density in units of $10^{27}\,m^{-3}$ and T_{keV} is the electron temperature in keV. The Nernst speed is therefore much smaller than v_η in liners in the WDM regime, where $n_{27} = 10^2$ and $T_{keV} = 10^{-3}$.

Slanting the post generates a supplemental axial field compared to straight posts. We are therefore increasing the inductance of the whole system. If the inductance becomes larger than the inductance of the configuration with Helmholtz coils, then the scheme proposed here would be penalizing. We can estimate the static axisymmetric inductance using

$$\int_V \frac{(B_\theta^2 + B_Z^2)}{2\mu_0} dV = \frac{1}{2}(L_\theta + L_Z) I^2. \tag{12}$$

We computed the ratio

$$L_Z/L_\theta = \int_V \frac{B_Z^2}{2\mu_0} dV \Big/ \int_V \frac{B_\theta^2}{2\mu_0} dV \tag{13}$$

using PERSEUS 60 ns into the current rise and the value came out to be 3.9%.

CONCLUSION

This work showed that resistivity gradients are a key mechanism in current penetration inside materials where warm dense matter cohabits with colder materials with much reduced resistivity. Non-linear diffusion forces current penetration along the direction antiparallel to resistivity gradients. This phenomenon is not symmetric, unlike linear diffusion. The current densities in MagLIF are certainly large enough to generate large resistivity gradients which will force currents to flow in regions of low resistivity. In our paper, we find that this region is the center of the liner wall, mid-way between both surfaces. This fast penetration could be an issue if the current reaches the inner surface of the liner early in the discharge, and causes ablation, mixing high-Z material from the wall with the low-Z fuel. However, we can also turn this mechanism to our advantage as we can now inject an external magnetic field into a liner on a time-scale much smaller than the skin time. The axial field generated by slanting the posts can replace the Helmholtz coil system altogether. Further considerations should be given to judge the efficiency of this scheme compared to MagLIF alternatives, such as Automag. This paper shows that the large axial field can penetrate the liner wall before the inner surface of the liner has started to move. By the time the fuel is heated by the laser, the required axial field should have fully penetrated the aluminum liner and the fuel. Under such conditions, the magnetic topology would be similar to the standard MagLIF scheme, without the use of external coils. The effects discussed herein would add to a substantial reduction of magneto-Rayleigh-Taylor instabilities caused by twisted return current paths.[14]

Since resistivity gradients are key in non-linear diffusion processes, the nature of the material is also an important control parameter. Going beyond pure substances, it seems possible to truly tailor the field penetration throughout the liner by using a multi-layer liner. Scientists could truly program field diffusion throughout the current discharge by using the appropriate material for each layer. If the field diffusion is chosen to be fast, then the current posts do not have to be twisted as much, reducing the overall inductance of the load. If the field diffusion is chosen to be slow, then the strength of the axial field can be increased by strongly slanting the posts. As a result, the axial field can also contribute to the implosion of the liner via JxB forces, while its penetration would be limited by the composite liner wall.

ACKNOWLEDGMENTS

The information, data, or work presented herein was funded in part by the Department of Energy National Nuclear Security Administration under Awards Nos. DE-SC0016252 and DE-NA0001944, the University of Rochester, the New York State Research and Development Authority, and the Advanced Research Projects Agency-Energy (ARPA-E), U.S. Department of Energy, under Award No. DE-AR000056. The views and opinions of authors expressed herein do not necessarily state or reflect those of the United States Government or any agency thereof.

[1]S. A. Slutz, M. C. Herrmann, R. A. Vesey, A. B. Sefkow, D. B. Sinars, D. C. Rovang, K. J. Peterson, and M. E. Cuneo, Phys. Plasmas **17**, 056303 (2010).
[2]J. D. Lawson, "Some Criteria for a Power producing thermonuclear reactor," Proc. Phys. Soc. London **B70**, 6 (1957).
[3]D. D. Ryutov, M. E. Cuneo, M. C. Herrmann, D. B. Sinars, and S. A. Slutz, Phys. Plasmas **19**, 062706 (2012).
[4]M. P. Desjarlais, Contrib. Plasma Phys. **41**, 267 (2001).
[5]H. M. Milchberg, R. R. Freeman, S. C. Davey, R. M. More, and Y. T. Lee, Phys. Rev. Lett. **61**, 2364 (1988).
[6]H. Knoepfel, *Pulsed High Magnetic Fields* (North Holland Publishing Company, 1970), p. 93.
[7]P.-A. Gourdain and C. E. Seyler, Phys. Rev. Lett. **110**, 015002 (2013).
[8]S. A. Slutz, C. A. Jennings, T. J. Awe, G. A. Shipley, B. T. Hutsel, and D. C. Lamppa, Phys. Plasmas **24**, 012704 (2017).
[9]C. E. Seyler and M. R. Martin, Phys. Plasmas **18**, 012703 (2011).
[10]R. D. McBride, M. R. Martin, R. W. Lemke, J. B. Greenly, C. A. Jennings, D. C. Rovang, D. B. Sinars, M. E. Cuneo, M. C. Herrmann, S. A. Slutz, C. W. Nakhleh, D. D. Ryutov, J.-P. Davis, D. G. Flicker, B. E. Blue, K. Tomlinson, D. Schroen, R. M. Stamm, G. E. Smith, J. K. Moore, T. J. Rogers, G. K. Robertson, R. J. Kamm, I. C. Smith, M. Savage, W. A. Stygar, G. A. Rochau, M. Jones, M. R. Lopez, J. L. Porter, and M. K. Matzen, Phys. Plasmas **20**, 056309 (2013).
[11]D. V. Knyazev and P. R. Levashov, Comput. Mater. Sci. **79**, 817 (2013).
[12]Z. Fu, W. Quan, W. Zhang, Z. Li, J. Zheng, Y. Gu, and Q. Chen, Phys. Plasmas **24**, 013303 (2017).
[13]J. R. Davies, R. Betti, P.-Y. Chang, and G. Fiksel, Phys. Plasmas **22**, 112703 (2015).
[14]P. F. Schmit, A. L. Velikovich, R. D. McBride, and G. K. Robertson, PRL **117**, 205001 (2016).